LETTERS

Strong effect of dispersal network structure on ecological dynamics

Matthew D. Holland[1] & Alan Hastings[1]

A central question in ecology with great importance for management, conservation and biological control is how changing connectivity affects the persistence and dynamics of interacting species. Researchers in many disciplines have used large systems of coupled oscillators to model the behaviour of a diverse array of fluctuating systems in nature[1–4]. In the well-studied regime of weak coupling, synchronization is favoured by increases in coupling strength and large-scale network structures (for example 'small worlds') that produce short cuts and clustering[5–9]. Here we show that, by contrast, randomizing the structure of dispersal networks in a model of predators and prey tends to favour asynchrony and prolonged transient dynamics, with resulting effects on the amplitudes of population fluctuations. Our results focus on synchronization and dynamics of clusters in models, and on timescales, more appropriate for ecology, namely smaller systems with strong interactions outside the weak-coupling regime, rather than the better-studied cases of large, weakly coupled systems. In these smaller systems, the dynamics of transients and the effects of changes in connectivity can be well understood using a set of methods including numerical reconstructions of phase dynamics, examinations of cluster formation and the consideration of important aspects of cyclic dynamics, such as amplitude.

Our study of the role of network structure on ecological dynamics considers exploiter–victim interactions[10–14] in networks that are relatively small and heterogeneous, and in which the importance of the amplitude of cycles means that results from weak coupling do not apply. We use explicit models of ecological dynamics, in which issues concerning both the phases and the amplitudes of oscillators are important, as opposed to general models based on phase oscillators[5,15]. The systems of conservation or ecological interest are typically those with strong connections[16], where boom-and-bust cycles can bring interacting populations close to extinction. Previous work suggests the importance of spatial structure and connectivity for reduction of cycle amplitude and increased persistence in both models[10–12,17,18] and laboratory systems[19]. More recently, great interest has arisen in the practical application of connectivity in a conservation context and in biological control[14], with all the heterogeneities present in natural and managed systems having a vital role[16,20–22]. However, most current theoretical understanding comes from models with very regular connections among patches, by contrast with the heterogeneity in natural systems that are far from regular[22–24]. We focus on heterogeneities, specifically in network structure, and on the formation of clusters, that is, groups of spatial locations with synchronous dynamics.

We present results for ten-patch systems, which are intermediate in size between typical studies of small systems (two to four patches[17,25]) and large lattice systems (hundreds to thousands of patches[4,12]). We choose this size mainly for tractability, and also because many managed systems have a relatively small number of connected sites, and larger systems behave similarly. We use regular lattices of degree four (each node, which represents a habitat patch, is connected to four nearest neighbours) to begin modelling dispersal networks. To investigate the effect of irregular patterns of dispersal among patches, we also consider networks that have been randomized by 'rewiring' one or more edges[26] (removing a connection between one pair of patches and replacing it with a connection between a different pair), as well as networks in which all edges (connections) have been assigned at random. Sample networks are shown in Fig. 1. The local and dispersal dynamics of the system are modelled as follows:

$$\frac{\mathrm{d}h_i}{\mathrm{d}t} = h_i(1-\theta h_i) - \frac{p_i h_i}{1+h_i} + d_h \sum_{j=1}^{n} A_{ij} h_j \qquad (1)$$

$$\frac{\mathrm{d}p_i}{\mathrm{d}t} = \frac{\phi p_i h_i}{1+h_i} - \eta p_i + d_p \sum_{j=1}^{n} A_{ij} p_j \qquad (2)$$

This is a non-dimensional and spatially structured form of the well-known Rosenzweig–MacArthur predator–prey model[27], with h representing prey density and p representing predator density, interacting in n discrete habitat patches[25]. The local dynamics are determined by three parameters: ϕ (prey-to-predator conversion rate), θ (strength of prey self-regulation) and η (predator mortality rate). Dispersal among patches is governed by the dispersal rates d_h (prey) and d_p (predators) and the matrix A.

The system of equations (1) and (2) can produce a variety of spatial dynamics. Solutions range from global synchrony (all patches display identical fluctuations through time; we will refer to this as the one-cluster solution) to global asynchrony (all patches have unique trajectories at any given time; n-cluster solutions), as well as solutions with between two and $n-1$ clusters of synchronous patches (Fig. 2 and Supplementary Figs 1–6). It is important to note that (even for the same parameter values) there may be several k-cluster solutions with different characteristics for $2 \leq k \leq n$. In particular, continuous measures of asynchrony such as correlation of densities among

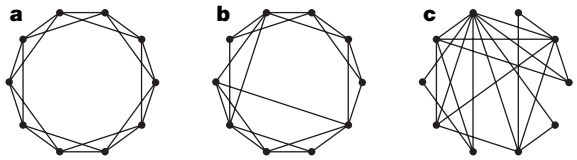

Figure 1 | Sample dispersal networks for systems with ten patches. All networks have an average degree of four, and dispersal is bidirectional. **a**, A ring lattice, referred to as a 'regular' network. **b**, A rewired ring lattice starts as a ring lattice and is rewired by replacing m edges at random. Here $m = 2$. **c**, A random network is produced by choosing $nk/2$ edges at random from all combinations of vertices (i, j) such that $i < j$. All dispersal networks used here were connected (every node can be reached by traversing one or more edges from every other node).

[1]Department of Environmental Science and Policy, University of California, Davis, One Shields Avenue, Davis, California 95616, USA.

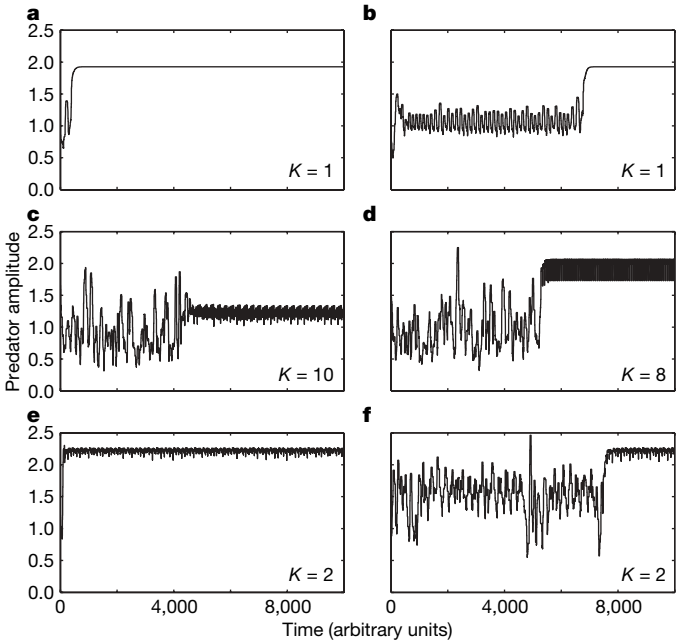

Figure 2 | Total predator amplitude (summed over all patches) as a function of time for cluster solutions. Local dynamics are characterized by strong prey density dependence ($\theta = 0.3$), predator mortality rates ($\eta = 1$) comparable to prey birth rates, moderate predator dispersal ($d_p = 2^{-7}$) and slower prey dispersal ($d_h = 2^{-9}$). **a, b,** Weak predation ($\phi = 2.75$) and regular networks. **c–f,** Strong predation ($\phi = 6$) and rewired networks ($m = 2$). All initial conditions and rewired networks were independently generated (see Methods). Each panel is labelled with the asymptotic number of clusters (K) observed in the simulation.

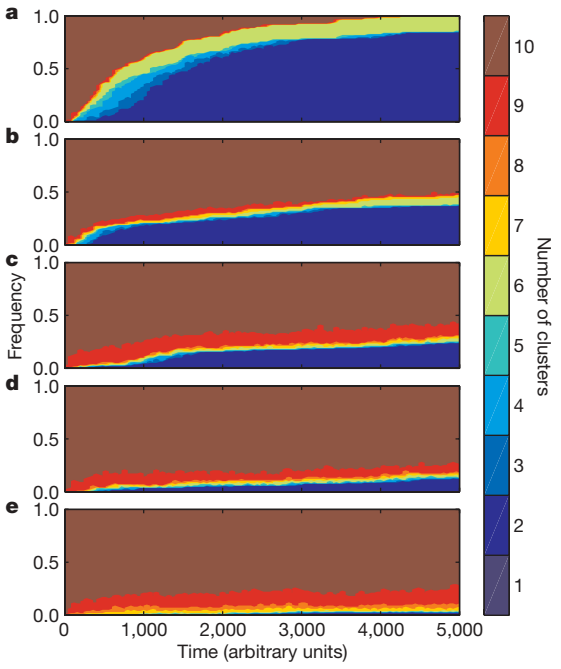

Figure 3 | Distribution of cluster states as a function of time. We consider systems with moderate dispersal rates ($d_h = 2^{-9}$, $d_p = 2^{-7}$) and ordered to random dispersal networks. **a**, Regular lattice; **b**, $m = 1$; **c**, $m = 2$; **d**, $m = 3$; **e**, random network. Regular networks converge to two- and six-cluster solutions, whereas irregular networks produce more eight-, nine- and ten-cluster solutions. Most of these large-k-cluster states are transient solutions. Local dynamics correspond to strong predation ($\phi = 5$), strongly self-regulating prey ($\theta = 0.3$) and predator mortality rates ($\eta = 1$) comparable to prey birth rates. Each panel summarizes 100 independent simulations.

patches in different clusters may vary among k-cluster solutions and over time for a single k-cluster solution. Thus, even 'globally asynchronous' n-cluster solutions may display considerable synchrony and, hence, larger amplitudes at various times during the solution. Furthermore, large-k-cluster classes can contain complex transient solutions resembling chaotic saddles, as well as asymptotic solutions displaying chaotic, quasi-periodic or periodic behaviour.

We find consistent and striking differences between dynamics with regular and irregular topologies for a broad range of underlying local dynamics. Looking at the distribution of cluster number through time in an ensemble of simulations reveals a substantial amount of information about the transient and asymptotic dynamics of these systems (Fig. 3 and Supplementary Figs 7–11). Increasing randomization of the network dramatically reduces the proportion of solutions with small to moderate numbers of clusters over ecologically relevant timescales.

For systems with heterogeneous dispersal networks, the temporal dynamics of k-cluster solutions suggest that transient dynamics are probably far more important than asymptotic dynamics on ecological timescales (Fig. 3). There are consequences for fluctuation amplitude and extinction risk of predators and prey, as is further revealed by manipulating both the local and the dispersal dynamics of the system. Varying predator efficiency, ϕ, is one way to move the system from low- to high-amplitude fluctuations. Because we are mainly interested in spatial persistence mechanisms, regional amplitude is a reasonable proxy for extinction risk in the context of a deterministic model (see Methods). For relatively low predator efficiencies, the asymptotic dynamics of all patch configurations are globally synchronous (Fig. 4a) and transients are short (Fig. 4b). At higher predator efficiencies, intermediate k-cluster solutions become stable, and asymptotic amplitudes level off near two orders of magnitude. This effect holds even at very high predator efficiencies, where single-patch systems fluctuate over five or more orders of magnitude and local extinction is extremely likely. The transient dynamics of these solutions have even lower median amplitudes, closer to one order of magnitude. Systems with irregular network structures spend much more time on these lower-amplitude transient solutions (Fig. 4b).

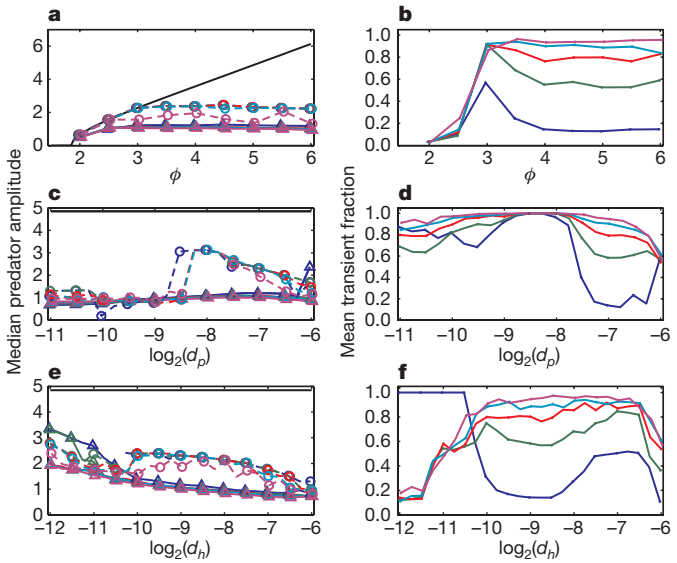

Figure 4 | Predator amplitude and transient duration. **a**, **c**, **e**, Median total predator amplitude during transient (triangles, solid lines) and asymptotic (open circles, dashed lines) solution phases; **b**, **d**, **f**, mean fraction of time spent in transient solutions. The black lines in **a**, **c**, and **e** are amplitudes of globally synchronous solutions for the chosen parameter values: $\theta = 0.3$, $\eta = 1$, $d_h = 2^{-9}$, $d_p = 2^{-7}$ (**a**, **b**); $\phi = 5$, $\theta = 0.3$, $\eta = 1$, $d_h = 2^{-9}$ (**c**, **d**), $\phi = 5$, $\theta = 0.3$, $\eta = 1$, $d_p = 2^{-7}$ (**e**, **f**). Data points are jittered horizontally and alternate markers omitted in **c–e** to improve readability. Each case uses at least 150 independent simulations. Dark blue, regular lattice; green, $m = 1$; red, $m = 2$; light blue, $m = 3$; pink, random network.

Manipulating dispersal rates leads to more complex spatio-temporal patterns. As predator dispersal is increased from a low value, we go from long transients and low-amplitude asymptotic solutions to a regime of higher amplitude asymptotic solutions preceded by lower-amplitude transients, with transient durations decreasing at higher movement rates (Fig. 4c, d). Very low values of prey dispersal produce shorter transients and low amplitudes in randomized networks and long transients of high amplitude in highly ordered lattices ($\log_2(d_h) < -10$; Fig. 4e, f). Larger rates of prey movement yield the now-familiar pattern of short transients leading to higher asymptotic amplitudes in ordered lattices, and longer transients of low amplitude in more disordered networks ($\log_2(d_h) > -10$, Fig. 4e, f).

Heterogeneous dispersal networks lead to dynamics with larger numbers of clusters (Fig. 3), which are generally transient solutions with considerable asynchrony and lower median amplitudes (Fig. 4) than the asymptotic solutions observed for lattice dispersal networks. There are some important caveats, however. Some transient solutions appear to be chaotic saddles or quasi-periodic solutions in which the median amplitude may not represent the dynamical regime that actually determines persistence. These solutions are relatively rare in our simulations, and occur most often for cases of strong resonance (Fig. 4c) or for very high values of predator dispersal (Supplementary Figs 14, 15). The relevance of such cases will of course depend on the details of the biological system being studied.

We demonstrate here that irregularities in connections among different sites in ecological networks can have large effects on the resulting dynamics. In particular, heterogeneous networks typically have longer periods of asynchronous dynamics, leading typically to lower amplitude fluctuations in population abundances; consequently, these are irregularities that cannot be ignored. However, decisions about the use of connectivity and corridors are being made in ecological systems based for the most part on theory that does not explicitly included heterogeneities[16,28]. Simultaneously, there is the need to characterize complex multidimensional systems in ecology, especially in the face of limited data. We show that for the kinds of systems we consider, cluster size is a simple, yet powerful and informative, way of characterizing dynamics, which both has a relationship to underlying network regularity and can help in understanding the dynamics of transient solutions on ecological timescales.

METHODS SUMMARY

The system of equations (1) and (2) was integrated numerically using a method appropriate for stiff equations. All simulations were initiated with pseudorandomly generated initial conditions, with all prey densities independently and identically distributed (i.i.d.) and all predator densities i.i.d. among all patches. For simulations using rewired or random networks, each simulation used an independently generated network.

Windowed analyses of cluster solutions (Fig. 3, Supplementary Figs 7–11) and amplitude (Figs 2, 4, Supplementary Figs 14, 15) were carried out on overlapping windows of length $4\bar{T}$ beginning at unit time intervals, where $\bar{T}$ is the mean period of a predator–prey cycle in a given simulation, averaged over all patches.

We defined a k-cluster solution as a solution in which the n patches in the system could be assigned to $k \leq n$ clusters of patches with identical dynamics. Clusters were taken to be the unions of all intersecting pairs of synchronous patches.

Time series were partitioned into transient and asymptotic regimes by treating predator–prey trajectories in individual patches as phase oscillators. We assumed that the rate of phase evolution within each patch would be constant when asymptotic dynamics had been reached. In fact, many of the asymptotic solutions contain periodic variation in the oscillator periods themselves. Thus, the transient phase of dynamics was defined as the interval of time before all patches displayed constant or periodic phase evolution. An automated algorithm (described in Methods) was used to estimate this value from numerical solutions to equations (1) and (2).

Total predator amplitude (Figs 2, 4) was defined simply as

$$\log_{10}\frac{\max\left(\sum_{i=1}^{n} p_i\right)}{\min\left(\sum_{i=1}^{n} p_i\right)}$$

over the time interval of interest, rather than as the greatest amplitude of any particular cycle in the interval.

Full Methods and any associated references are available in the online version of the paper at www.nature.com/nature.

Received 17 July; accepted 5 September 2008.
Published online 19 October 2008.

1. Winfree, A. T. *The Geometry of Biological Time* (Springer, 1980).
2. Kuramoto, Y. *Chemical Oscillations, Waves, and Turbulence* (Springer, 1984).
3. Izhikevich, E. M. *Dynamical Systems in Neuroscience: The Geometry of Excitability and Bursting* (MIT Press, 2007).
4. Blasius, B., Huppert, A. & Stone, L. Complex dynamics and phase synchronization in spatially extended ecological systems. *Nature* **399,** 354–359 (1999).
5. Acebrón, J. A., Bonilla, L. L., Pérez Vicente, C. J., Ritort, F. & Spigler, R. The Kuramoto model: A simple paradigm for synchronization phenomena. *Rev. Mod. Phys.* **77,** 137–185 (2005).
6. Watts, D. J. *Small Worlds* (Princeton Univ. Press, 1999).
7. Barahona, M. & Pecora, L. M. Synchronization in small-world systems. *Phys. Rev. Lett.* **89,** 054101 (2002).
8. Hong, H., Choi, M. Y. & Kim, B. J. Synchronization on small-world networks. *Phys. Rev. E* **65,** 026139 (2002).
9. Nishikawa, T., Motter, A. E., Lai, Y. C. & Hoppensteadt, F. C. Heterogeneity in oscillator networks: Are smaller worlds easier to synchronize? *Phys. Rev. Lett.* **91,** 014101 (2003).
10. Hassell, M. P. & May, R. M. Aggregation of predators and insect parasites and its effect on stability. *J. Anim. Ecol.* **43,** 567–594 (1974).
11. Crowley, P. H. Dispersal and the stability of predator-prey interactions. *Am. Nat.* **118,** 673–701 (1981).
12. Comins, H. N. & Hassell, M. P. Persistence of multispecies host-parasitoid interactions in spatially distributed models with local dispersal. *J. Theor. Biol.* **183,** 19–28 (1996).
13. Ellner, S. P. *et al.* Habitat structure and population persistence in an experimental community. *Nature* **412,** 538–543 (2001).
14. Murdoch, W. W., Briggs, C. J. & Nisbet, R. M. *Consumer-Resource Dynamics* (Princeton Univ. Press, 2003).
15. Matthews, P. C., Mirollo, R. E. & Strogatz, S. H. Dynamics of a large system of coupled nonlinear oscillators. *Physica D* **52,** 293–331 (1991).
16. Crooks, K. R. & Sanjayan, M. A. *Connectivity Conservation* (Cambridge Univ. Press, 2006).
17. Jansen, V. A. A. The dynamics of two diffusively coupled predator-prey populations. *Theor. Popul. Biol.* **59,** 119–131 (2001).
18. Hudgens, B. R. & Haddad, N. M. Predicting which species will benefit from corridors in fragmented landscapes from population growth models. *Am. Nat.* **161,** 808–820 (2003).
19. Holyoak, M. Habitat patch arrangement and metapopulation persistence of predators and prey. *Am. Nat.* **156,** 378–389 (2000).
20. Urban, D. & Keitt, T. Landscape connectivity: a graph-theoretic perspective. *Ecology* **82,** 1205–1218 (2001).
21. Tewksbury, J. J. *et al.* Corridors affect plants, animals, and their interactions in fragmented landscapes. *Proc. Natl Acad. Sci. USA* **99,** 12923–12926 (2002).
22. Fortuna, M. A., Gómez-Rodriguez, C. & Bascompte, J. Spatial network structure and amphibian persistence in stochastic environments. *Proc. R. Soc. Lond. B* **273,** 1429–1434 (2006).
23. Hanski, I. & Ovaskainen, O. The metapopulation capacity of a fragmented landscape. *Nature* **404,** 755–758 (2000).
24. McIntire, E. J. B., Schultz, C. B. & Crone, E. E. Designing a network for butterfly habitat restoration: where individuals, populations and landscapes interact. *J. Appl. Ecol.* **44,** 725–736 (2007).
25. Hastings, A. Transient dynamics and persistence of ecological systems. *Ecol. Lett.* **4,** 215–220 (2001).
26. Watts, D. J. & Strogatz, S. H. Collective dynamics of 'small-world' networks. *Nature* **393,** 440–442 (1998).
27. Rosenzweig, M. L. & MacArthur, R. H. Graphical representation and stability conditions of predator-prey interactions. *Am. Nat.* **97,** 209–223 (1963).
28. Hilty, J. A., Lidicker, W. Z. & Merenlender, A. M. *Corridor Ecology: The Science and Practice of Linking Landscapes for Biodiversity Conservation* (Island Press, 2006).

Supplementary Information is linked to the online version of the paper at www.nature.com/nature.

Acknowledgements We thank M. Holyoak for comments on an earlier version of the manuscript and D. Wysham for discussions. M.D.H. was funded by a Quantitative Environmental and Integrative Biology grant to A.H. and M. Holyoak from the National Science Foundation.

Author Contributions M.D.H. wrote custom software, ran simulations and analyzed data. M.D.H. and A.H. designed the study and wrote the paper.

Author Information Reprints and permissions information is available at www.nature.com/reprints. Correspondence and requests for materials should be addressed to M.D.H. (mdholland@ucdavis.edu).

METHODS

Numerical integration. Numerical integration was carried out using the backward-differentiation formula method in CVODE (ref. 29). Prey initial conditions were i.i.d. with $\log_{10}(h_i(0))$ uniformly distributed on the interval $(-5, 1+\log_{10}\hat{\boldsymbol{h}})$ and predator initial conditions were i.i.d. with $\log_{10}(p_i(0))$ uniformly distributed on the interval $(-5, 1+\log_{10}\hat{\boldsymbol{p}})$, where $\hat{\boldsymbol{h}} = \eta/(\phi-\eta)$ and $\hat{\boldsymbol{p}} = (1+\hat{\boldsymbol{h}})(1-\theta\hat{\boldsymbol{h}})$.

Dispersal networks. We used three types of dispersal networks (Fig. 1), all with an average number of connections per vertex (degree) of four. A ring lattice of degree four (Fig. 1a) is obtained by placing n points on a ring and connecting each to its four nearest neighbours. A rewired ring lattice (Fig. 1b) is obtained by deleting m randomly chosen edges from a ring lattice and replacing them at random. Because our networks are small, we chose random edges from the set of edges not included in the original lattice. We generated random graphs of degree four (Fig. 1c) by choosing $2n$ edges at random from the $n(n-1)/2$ possible undirected edges. All networks were connected (every vertex can be reached by traversing one or more edges from every other vertex).

Pseudorandom number generation. Pseudorandom numbers were generated using the Mersenne twister algorithm.

Cluster identification. Dynamics in pairs of patches were compared by calculating the linear correlation coefficient, ρ_{ij}, of prey time series in all pairs of patches. A pair of patches was taken to have identical dynamics, and thus assigned to the same cluster, if $\rho_{ij} > 0.999$.

Non-dimensionalization. The system of equations (1) and (2) was obtained by non-dimensionalizing a spatially explicit version of the Rosenzweig–MacArthur[27] equations

$$\frac{\mathrm{d}H_i}{\mathrm{d}\tau} = H_i\left(1-\frac{H_i}{K}\right) - \frac{aP_iH_i}{b+H_i} + D_H\sum_{j=1}^{n}A_{ij}H_j$$

$$\frac{\mathrm{d}P_i}{\mathrm{d}\tau} = \frac{caP_iH_i}{b+H_i} - mP_i + D_P\sum_{j=1}^{n}A_{ij}P_j$$

by making the substitutions $h_i = H_i/b$, $p_i = aP_i/rb$ and $t = r\tau$ and defining the parameters $\theta = b/K$, $\phi = ca/r$, $\eta = m/r$, $d_h = D_H/r$ and $d_p = D_P/r$. The matrix $A = M - E$ represents the allowed dispersal transitions, where M is the adjacency matrix of the dispersal network, meaning that $M_{ij} = 1$ if individuals are allowed to move from patch j to patch i. E represents emigration, and is thus a diagonal matrix with entries $E_{ii} = \sum_{j=1}^{n} M_{ji}$.

Phase analysis of transient duration. Phase dynamics of solutions to the predator–prey model in equations (1) and (2) were reconstructed by treating the projections of the solution into the planes $h_i \times p_i$ as phase plane trajectories of limit cycle oscillators. The time between subsequent crossings from above of the line segment connecting the nontrivial equilibrium at $(\hat{\boldsymbol{h}}, \hat{\boldsymbol{p}})$ to the origin was taken to represent one cycle, or 2π radians of phase evolution. We defined $Z_i = f(T_i) - \overline{f(T_{i,\alpha})}$, where $T_i = T_{i,1}, T_{i,2}, \ldots, T_{i,j}, \ldots, T_{i,N}$ is the time series of N cycle periods in the ith patch, f is a low-pass filter and $T_{i,\alpha}$ is the series of periods in the ith patch for the last αN observations of T_i. Thus, the elements Z_i should be close to zero when asymptotic dynamics have been reached. In practice, it is necessary to choose a positive threshold, ε, and declare that asymptotic dynamics have been reached by time k if $|Z_i| < \varepsilon$ for all $j > k$. Errors can result when the asymptotic dynamics of one or more patches are poorly approximated by a simple limit cycle, but if these deviations are themselves periodic at high frequencies, they will be removed by the filter f. Most commonly, the one or two lowest amplitude patches will have sufficiently slow variation in period to cause errors. Therefore, in addition to filtering the T_i to obtain Z_i, we estimated the transient duration as the time until at least eight of ten patches had reached the stage of asymptotic behaviour by the above criterion, with $\varepsilon = 0.1$ and $\alpha = 0.167$.

The filter f was chosen to be a (Blackman) windowed sinc filter[30] with 151 points and a cut-off frequency of 0.05 per sample. This filter has a transition band from 0.04 (0-dB amplitude gain) to 0.07 per sample (-74-dB amplitude gain). In practice, this means that large-period deviations occurring on timescales of 14 or more cycles may remain in the Z_i, causing us to incorrectly conclude that asymptotic dynamics are never reached. The solution shown in Supplementary Figs 1i, 2i, 3i is an example of such a case.

29. Cohen, S. D. & Hindmarsh, A. C. CVODE, a stiff/nonstiff ODE solver in C. *Computers Phys.* **10**, 138–143 (1996).
30. Smith, S. W. *The Scientist and Engineer's Guide to Digital Signal Processing* (California Technical Publishing, 1997).